

## Photochemical Generation of Electrons and Holes in Germanium-Containing ITQ-17 Zeolite

Mercedes Alvaro, Pedro Atienzar, Avelino Corma,\* Belén Ferrer, Hermenegildo Garcia,\* and Maria T. Navarro

*Instituto de Tecnología Química CSIC-UPV and Departamento de Química, Universidad Politécnica de Valencia, Avenida de los Naranjos s/n, 46022 Valencia, Spain*

*Received: July 1, 2004; In Final Form: December 10, 2004*

Laser flash photolysis of germanium-containing ITQ-17 zeolite (Ge/ITQ-17, a single polymorph of  $\beta$  zeolite) at 266 nm generates a transient spectrum decaying in the sub-millisecond time scale that is compatible with the formation of two transient species. The shorter lived transient ( $\tau \approx 45 \mu\text{s}$  under nitrogen) has been assigned to trapped electrons due to the characteristic spectroscopic absorption (single band at 480 nm) and its quenching by typical electron scavengers such as  $\text{N}_2\text{O}$  and  $\text{CH}_2\text{Cl}_2$ . The second longer lived transient ( $\lambda_{\text{max}} = 500, 540,$  and  $600 \text{ nm}$ ;  $\tau \approx 390 \mu\text{s}$ ) is not quenched by  $\text{O}_2$  or electron scavengers, but it is quenched by methanol as hole scavenger and has been assigned to positive holes. Also there is a remarkable similarity of the transient spectrum of the Ge/ITQ-17 with the optical spectrum reported previously for electron–hole pairs in ZSM-5 zeolite. Under the same irradiation conditions, photoejection of electrons and photogeneration of positive holes has not been observed for conventional aluminosilicate zeolites, all-silica zeolites, or  $\text{GeO}_2$ -impregnated zeolites. Therefore this photochemical behavior has been ascribed to the presence of framework germanium atoms opening the way for photoresponsive zeolites. The ability of Ge/ITQ-17 to generate photochemically electrons and holes has been confirmed by adsorbing naphthalene and propyl viologen sulfonate as electron donor and acceptor, respectively, and observing the generation of the corresponding radical ions.

## Introduction

Aluminum-containing zeolites are among the most important solid acid catalysts, and an enormous number of articles has been published reporting their synthesis, the structure, nature, and strength of their acid sites, and catalytic properties.<sup>1,2</sup> The preparation and properties of zeolites containing other heteroatoms is also a subject of much current interest, particularly for their application in heterogeneous catalysis.<sup>3</sup>

Although crystalline, microporous germanosilicates have been known from a long time ago,<sup>4–8</sup> their importance compared to aluminosilicate analogues is relatively minor since they do not exhibit activity as solid acids. However, there is a renewed interest in germanium-containing zeolites since we have recently developed a new concept in zeolite synthesis based on the effect as a structure-directing agent of the incorporation of germanium in the framework.<sup>9–11</sup> Germanium being an element of the same family as silicon can replace a certain percentage of silicon in the zeolite structure, but the larger germanium atomic radius introduces more framework flexibility and a higher tolerance in the crystal structure to acute bond angles, favoring the presence of four-membered rings in the zeolite primary building blocks. The presence of three- and four-membered rings is a prerequisite in the synthesis of large- and extralarge-pore zeolites, a long-pursued task.<sup>12</sup> Thus, the presence of germanium in the synthesis gel can promote the crystallization of zeolitic structures different from those formed in its absence. One example of the germanium structure-directing effect is the case of the synthesis of zeolite ITQ-17, a single polymorph Si of  $\beta$  zeolite.<sup>13</sup>

In the field of supramolecular chemistry, zeolites have also attracted interest in photochemistry as a rigid media to alter and control the properties of incorporated guests.<sup>14</sup> While, in some cases, the zeolite framework plays a *passive* role merely

defining a compartmentalized space, in some other reported examples, particularly in charge-transfer (CT) and photoinduced electron-transfer (ET) processes, it has been found that the zeolite framework can play an *active* role in accepting or donating electrons.<sup>14–16</sup> Since germanium is less electronegative than silicon, oxygen atoms in germanosilicates have a higher electron density than in conventional silicate zeolites, and hence, we anticipated that its presence could enhance the ability of the zeolite framework to participate in CT and photoinduced ET processes.

Herein we report a laser flash photolysis study of the pristine ITQ-17 germanosilicate in which upon photoexcitation we have observed an enhanced tendency to undergo charge separation, with the generation of electrons and holes decaying in the sub-millisecond time scale. This behavior is not observed under the same conditions in analogous zeolites lacking germanium atoms.

## Results and Discussion

Aluminosilicates do not absorb in the UV region above 200 nm. The presence of framework germanium atoms introduces a new absorption band at  $\lambda_{\text{max}} = 225 \text{ nm}$ , corresponding to the  $-\text{O}-\text{Ge}\equiv$  ligand-to-metal charge transfer.<sup>17</sup> Figure 1 presents the diffuse reflectance UV–vis (DR UV–vis) spectrum of as-synthesized Ge/ITQ-17 in which, in addition to the framework CT  $-\text{O}-\text{Ge}\equiv$  absorption band at 225 nm, a peak due to the organic *N*-benzyl 1,4-diazabicyclo[2.2.2]octane (DABCO) used as a template in the synthesis of the zeolite appearing at 265 nm is also observed. Upon adequate calcination treatment, the organic template is completely removed according to combustion chemical analyses and, accordingly, the band at 265 nm disappears, while the  $-\text{O}-\text{Ge}\equiv$  band, although blue-shifted and broader, is still observed.

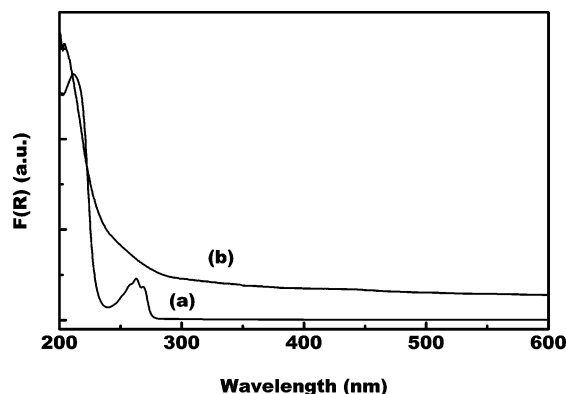


**Figure 1.** DR UV-vis spectrum (plotted as the Kubelka–Munk function of the reflectance,  $R$ ) of Ge/ITQ-17: (a) as-synthesized sample containing *N*-benzyl DABCO template ( $\lambda_{\text{max}} = 265$  nm) and (b) after calcination. The absorption peak at 225 nm is characteristic of the  $\text{—O—Ge}\equiv$  chromophore.

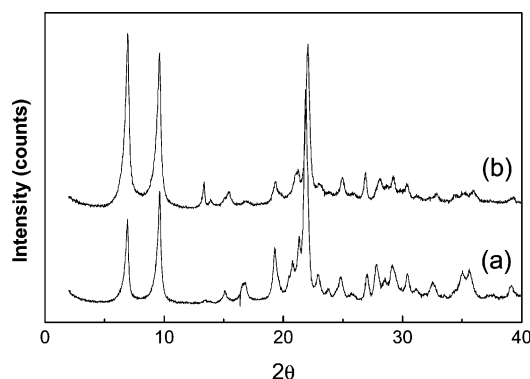


**Figure 2.** Powder X-ray diffraction of Ge/ITQ-17 (Si/Ge 3.5) before (a) and after (b) template removal.

Removal of the organic template by calcination was carried out by slow gradual temperature increase, first under a nitrogen flow and later under dry air to minimize the out-of-framework migration of germanium during the process. The presence of moisture in the calcination process or postcalcination storage is believed to play an adverse role, promoting migration of Ge from framework to out-of-framework positions. Nevertheless it is worth a reminder that formation of nonframework species during calcination is a general phenomenon that occurs in different degrees not only in germanosilicates but also in most of the zeolites including those containing aluminum.<sup>18–23</sup> Thus, appearance of octahedral Al (out-of-framework) upon calcination of zeolite samples containing exclusively tetrahedral Al (framework positions) has been firmly demonstrated by solid-state  $^{27}\text{Al}$  NMR spectroscopy, recording the spectrum before (single Al peak at 52 ppm) and after calcination (peak at 110 ppm in addition to that at 52 ppm). In the case of ITQ-17 germanosilicate, the formation of nonframework germanium can be simply assessed by the presence of a broad, low intense absorption band from 400 to 250 nm. To illustrate this point, Figure 1 also plots the DR UV-vis spectrum of calcined Ge/ITQ-17. This migration is also reflected in a decrease in the intensity of the powder X-ray diffraction pattern of the zeolite before and after calcination (Figure 2). As in the case of other heteroatoms, the framework to out-of-framework migration is more pronounced as the germanium content of the zeolite increases. In any case, Figure 2 clearly shows that calcined Ge/ITQ-17 still retains over 85% of the initial crystallinity. For our laser flash photolysis study we have used a calcined Ge/ITQ-17 sample with a Si/Ge atomic ratio of 3.5.

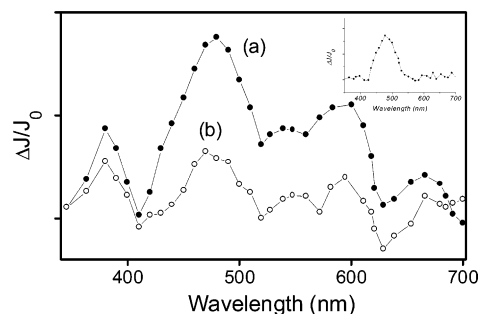


**Figure 3.** Transient DR spectra recorded at 10 (a) and 100  $\mu\text{s}$  (b) after the laser excitation. The inset shows the spectrum difference between the transient recorded at 2 and 10  $\mu\text{s}$ .

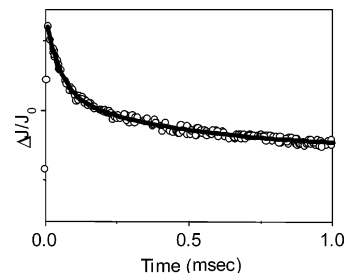


**Figure 4.** Signal decay monitored at 480 nm after 266 nm laser excitation, fitted to a two-term first-order kinetics with half-lives of 45 and 390  $\mu\text{s}$  and relative intensities of 40 and 60%, respectively.

The presence of CT  $\text{—O—Ge}\equiv$  absorption band renders germanosilicates photochemically active upon excitation at this band. We have previously reported the photoluminescence of germanium-containing zeolites arising from this ligand-to-metal electronic transition,<sup>24</sup> and now we want to show that, in addition to photoluminescence, photochemical excitation is also able to produce charge separation with formation of electron and holes to some extent.

Laser excitation of calcined Ge/ITQ-17 samples at the CT  $\text{—O—Ge}\equiv$  band was accomplished by using the fourth harmonic ( $\lambda = 266$  nm) of the primary frequency of a Nd:YAG laser. The corresponding transient DR spectra recorded at two different delays after the laser flash are shown in Figure 3 and consist in a continuous absorption exhibiting relative absorption maxima at 380, 480, 540, 600, and 660 nm. That the origin of this transient is the framework  $\text{—O—Ge}\equiv$  chromophores is supported by the fact that 266 nm excitation under the same conditions of a series of conventional aluminosilicate zeolites taken as controls does not allow one to record the generation of any transient. Furthermore, blanks in which germanium oxide were deposited on zeolites do not allow one to record any transient.

The transient spectrum shown in Figure 3 plot a corresponds to more than a single species since the signal temporal profile varies with the wavelength. The temporal profile of the signal measured at 480 nm (the most intense absorption band) can be fitted to a two consecutive first-order kinetics. To give a visual indication of the quality of the kinetic data, Figure 4 shows the 480 nm signal temporal profile and the theoretical two-term first-order fitting from which the kinetic parameters have been obtained. The respective half-lives for the two consecutive first-order kinetics were estimated to be 45 and 390  $\mu\text{s}$  and their relative intensities were 40 and 60%, for the fast and slow decay, respectively. Alternative equations using a second-order kinetics fit significantly worse to the experimental points.

Normally the decay kinetics in heterogeneous media are better described by constructing a stretched decay following the signal

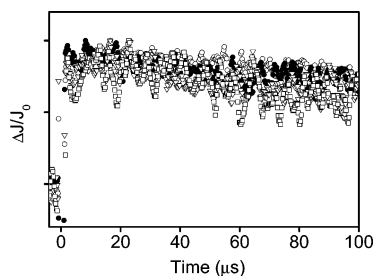


**Figure 5.** Normalized temporal profiles monitored at long time scales for 390 (○), 480 (●), 550 (▽), and 660 nm (□) after a 266 nm laser excitation of calcined Ge/ITQ-17.

in several time scales.<sup>25</sup> In the case considered here, the maximum time window available to our diffuse reflectance nano-second setup spans from 100 ns to 1 ms. Slow response time is a common characteristic of diffuse reflectance techniques as compared to faster transmission measurements,<sup>26</sup> and this precludes study of shorter time scales, while laser flash photolysis being a fast kinetic technique cannot usually monitor longer than milliseconds. This is the time window presented in Figures 4 and 6.

The temporal profile measured at 480 nm did not change with the laser power in the range 5–30 mJ·pulse<sup>-1</sup>, while the signal intensity follows a linear relationship with the laser intensity. These two observations indicate that we are dealing with a monophotonic event, that gives rise to the photogenerated species in the same proportion through the whole laser power range.

There are two simple explanations for the temporal profile monitored at 480 nm: either (i) there are two different species absorbing in the same spectral region, but decaying with different lifetimes, or (ii) there is a single species decaying with two different mechanisms.

If the kinetic data shown in Figure 4 would correspond to two species, one of them decaying much faster than the other, then the transient spectrum recorded at long delay times, when the first species has completely decayed, should correspond to the longer lived single species. This spectrum recorded 100 μs after the laser pulse is also shown in Figure 3 (plot b). In support that the spectrum recorded at this delay time corresponds to a single species, Figure 5 shows that the normalized temporal profiles monitored at the 100 μs time scale are coincident at all the wavelengths of the spectrum.

However, there is still the possibility not ruled out by the kinetic data that the decay at 480 nm would correspond to a single species decaying with two different regimes and that the slower regime coincides with the temporal profile of other transient species. It has to be noted that the signal monitored at 480 nm has a fast component that is not observed at any of the other wavelengths (see also Figure 6).

To assess the nature of the two different species generated upon photoexcitation, we performed quenching experiments. The presence of oxygen does not influence the decay, ruling out the implication of triplet states as being responsible for any of the transients. N<sub>2</sub>O and CH<sub>2</sub>Cl<sub>2</sub> were selected as typical quenchers for ejected electrons due to the experimental simplicity of their adsorption onto the zeolite powder from the gas phase. In contrast to the lack of influence by the presence of oxygen, N<sub>2</sub>O and CH<sub>2</sub>Cl<sub>2</sub> notably influence the decay of the shorter lived transient that eventually disappears under these conditions, leaving an unquenchable residual signal (Figure 6). Also, these two quenchers do not affect at all the temporal profile of the longer lived transient (Figure 6). The transient

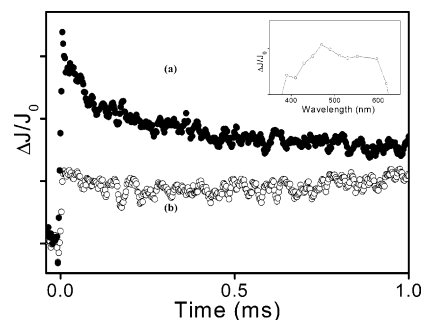


**Figure 6.** Temporal profile of the signal monitored at 480 nm after 266 nm excitation of Ge/ITQ-17 monitored in atmosphere of N<sub>2</sub> (a) and atmosphere of N<sub>2</sub>O (b). The inset shows the transient spectrum recorded 1 μs after 266 nm for a Ge/ITQ-17 sample purged with a CH<sub>2</sub>Cl<sub>2</sub>-saturated N<sub>2</sub> flow.

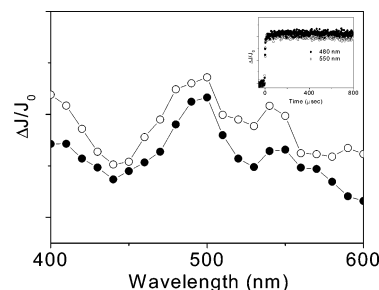


**Figure 7.** Transient spectra recorded 10 (○) and 100 μs (●) after 266 nm laser excitation of Ge/ITQ-17 purged 5 or 15 min with a methanol-saturated N<sub>2</sub> flow. The inset shows normalized decays monitored at 480 and 540 nm.

spectrum recorded after extensive N<sub>2</sub>O purging and therefore presumably devoid of ejected electrons is also shown as an inset in Figure 6. Note that the presence of a residual absorption at 480 nm supports that, in addition to ejected electrons, there is also a population of unquenchable electrons or other species absorbing in this wavelength. Moreover, the effect of the quenchers was reversible, and the shorter lived transient signal is restored when the Ge/ITQ-17 sample is exhaustively purged with N<sub>2</sub> gas.

We also supported independently the formation of holes upon photoexcitation of Ge/ITQ-17 by purging the sample with methanol. Methanol acts as a hole scavenger leaving framework and solvated electrons. In accordance with our expectancies, purging Ge/ITQ-17 with methanol-saturated N<sub>2</sub> at room temperature for sufficient time leads to a significant decrease of the 600 nm absorbance and a broadening of the 480 nm absorption (Figure 7). In this case the effect of methanol addition was not reversible and N<sub>2</sub> purging was not sufficient to revert to the original transient spectrum recorded in the absence of methanol. It seems, however, that methanol is not absolutely clean as quencher, and some photoproducts are formed.

Finally we proceeded to incorporate to solid organic compounds into Ge/ITQ-17, namely, naphthalene (NP) and propyl viologensulfonate (PVS). When entrapped inside zeolites, NP is a good electron donor, and upon excitation it could generate NP<sup>•+</sup> radical cation and electrons.<sup>15,27</sup> As shown in Figure 8, the transient spectrum recorded 100 μs after 266 nm laser excitation is compatible with the generation of NP<sup>•+</sup> (λ<sub>max</sub> = 580–630 nm) and electrons that exhibit the characteristic absorption band at 480 nm compatible with the absorption band recorded in the direct excitation of Ge/ITQ-17.

Analogously, the transient spectrum recorded for PVS included inside Ge/ITQ-17 corresponds basically to PVS<sup>•-</sup> radical anion (Figure 9). Although observation of PVS<sup>•-</sup> is

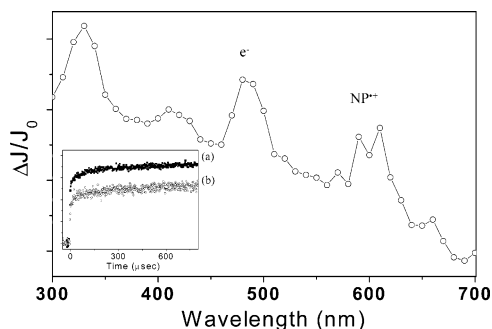


**Figure 8.** Transient spectrum recorded 100  $\mu$ s after 266 nm laser excitation of a  $N_2$ -purged Ge/ITQ-17 containing NP. The characteristic peaks of  $NP^{\bullet+}$  and electrons have been indicated in the figure. The inset shows the signal temporal profile monitored at 480 (a) and 610 nm (b), respectively.

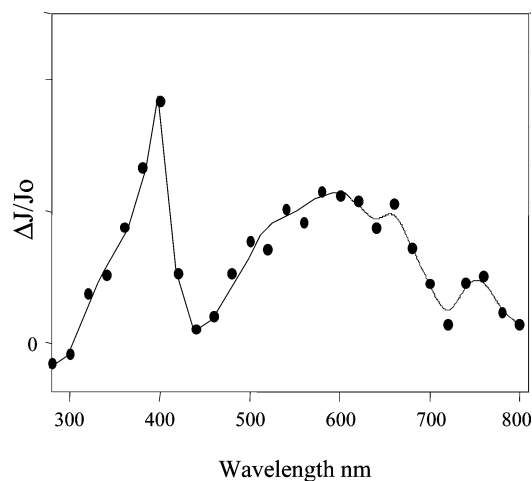
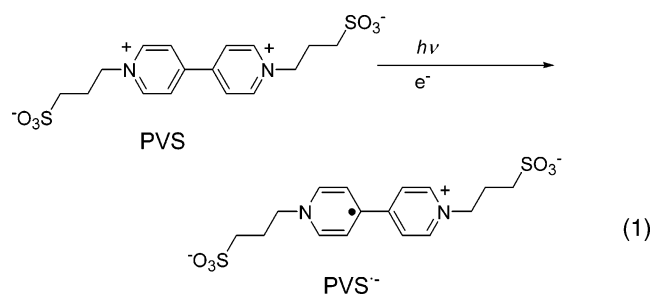


**Figure 9.** Transient spectrum recorded 100  $\mu$ s after upon 266 nm laser excitation of a  $N_2$ -purged sample of Ge/ITQ-17 containing PVS.

evidence that electron donation from the zeolite framework to PVS has occurred as indicated in eq 1, it is unfortunate that the large absorptivity of  $PVS^{\bullet-}$  obscures the observation of zeolite holes.



The observed quenching behavior of the short-lived transient and the 480 nm band in the transient spectrum of NP incorporated inside Ge/ITQ-17 are compatible with the presence of photoejected electrons. The fact that Moissette et al. have

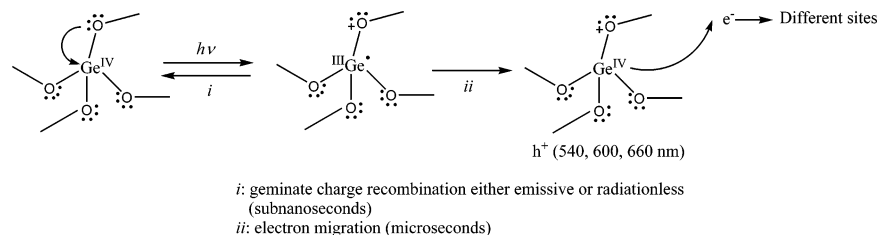
reported that photoejected electrons in ZSM-5 devoid of alkali metal ions are characterized by a single absorption band at 480 nm is in agreement with our interpretation.<sup>28</sup> However, typical electron scavengers such as  $N_2O$  and  $CH_2Cl_2$  only quench in part the signal at 480 nm, indicating that there is a contribution of other species or unquenchable electrons to the 480 nm band observed in Figure 3. What is firmly supported is that the absorption difference between our spectra recorded at short and long delay times and between  $N_2O$  or  $CH_2Cl_2$  quenched or unquenched spectra corresponds to photoejected electrons.

Considering that charge separation through ligand-to-metal electron transfer is a general phenomenon in semiconductor metal oxides<sup>17</sup> that has already been claimed to be involved in the photoluminescence of germanium silicates<sup>24</sup> and that the presence of ejected electrons is compatible with the short-lived transient behavior, the most probable nature of the longer lived transient would correspond to positive holes or to a charge-separated state consisting of electron–hole pairs. In fact, the transient spectrum recorded at long delay time resembles that recorded for electron–hole pairs in aluminosilicate zeolites.<sup>27,29,30</sup> However, it is obvious that Ge/ITQ-6 may have characteristic absorption bands in the transient spectra centered on germanium atoms that are not present in aluminosilicate zeolites.

According to this, Scheme 1 provides a simple rationalization of the photochemistry observed for Ge/ITQ-17. In this scheme, photoexcitation of the  $-O-Ge\equiv$  chromophore would produce electron transfer from the oxygen to the germanium atom. The charge-separated state could decay by back-electron transfer from  $Ge^{III}$  to  $-O(\bullet+)-$  in geminate pairs (process i in Scheme 1), this process occurring in the subnanosecond time scale and not being observable by us. Alternatively, in some cases the electron on the germanium atom would migrate and become delocalized in the zeolite framework and pore space (process ii). Also hole migration can take place by electron hopping between neighbor oxygens. This leads to a charge-separated state that would decay by a non-geminate recombination pathway and would be spectroscopically detectable at longer time scales.

In principle, if the process being observed in the time window of our study (between 1 and 100  $\mu$ s) was electron and hole recombination, the signal should decay following a second-order kinetics with the same rate constant over the wavelength range. Clearly the temporal profile of our signal at any wavelength does not fit to a second-order kinetics, thus ruling out electron–hole recombination as the process being observed. In addition, the temporal profile also changes depending on the wavelength being monitored. These facts are compatible with the occurrence of electron and hole migration as the most probable process occurring in our time scale. Electron hopping between different acceptor sites inside zeolite  $Na-Y$  is a process that has been determined to occur in hundreds of microseconds. Then, one possibility would be that photogenerated electrons and holes move and distribute among sites different from the original  $\equiv Ge^{III}-O-$  charge-separated state, the spectroscopic character-

#### SCHEME 1: Rationalization of the Photochemistry Observed for Ge/ITQ-17





istics of each site being different. For instance, while electrons in dealuminated Na ZSM-5 are reported as a band at 480 nm,<sup>28</sup> hydrated electrons exhibit a very broad, continuous absorption starting in 600 nm and having a maximum beyond 800 nm with different extinction coefficient, and, therefore, the spectra of these two electron types are different. The same may happen in our Ge/ITQ-17, where a wide distribution of sites inherent to any zeolite should be present. Our hypothesis is summarized in Scheme 1.

In summary, by means of laser flash photolysis studies we have shown that germanium-containing zeolites are interesting materials due to their photoactivity, which can be rationalized as arising from a photoinduced charge separation, with the generation of ejected electrons and holes. This photochemical behavior of Ge-containing zeolites sharply contrasts with the lack of photoactivity of all-silica or aluminum-containing zeolites under the same conditions and opens the way to potential applications of zeolites in photovoltaic cells and photoresponsive electronics.

### Experimental Section

Ground-state diffuse reflectance UV–vis spectra were recorded on a Cary 5G using a praying mantis accessory for solids and using BaSO<sub>4</sub> as standard. Laser flash photolysis experiments were carried out using the fourth (266 nm, 20 mJ·pulse<sup>-1</sup>) harmonic of a Surelite Nd:YAG laser for excitation (pulse ≤ 10 ns). The signal from the monochromator/photomultiplier detection system was captured by a Tektronix TDS640A digitizer and transferred to a PC computer that controlled the experiment and provided suitable processing and data storage capabilities. Fundamentals<sup>31</sup> and details<sup>25</sup> of a similar time-resolved laser setup have been published elsewhere. NP was a commercial sample and was recrystallized from ethanol before adsorption. PVS was synthesized by reacting 4,4'-bipyridine and sultone in ethanol at reflux temperature.

**Preparation of Zeolite Ge/ITQ-17.** a Ge-containing ITQ-17 was synthesized by using the hydroxide form of benzyl-DABCO (BD<sup>+</sup>) as structure-directing agent. The synthesis gel was prepared with the following molar composition: 0.833:0.166:0.5:0.5:8 SiO<sub>2</sub>:GeO<sub>2</sub>:BDOH:HF:H<sub>2</sub>O. This was obtained by adding GeO<sub>2</sub> (powder) and TEOS (tetraethyl orthosilicate) to an aqueous solution of BDOH. The homogeneous mixture was stirred vigorously at room temperature to eliminate the ethanol produced during the hydrolysis. The resulting gel was introduced into a Teflon-lined stainless steel autoclave and was heated at 150 °C for 15 h under static conditions. The solid was recovered by filtration and then was extensively washed with distilled water and dried at 100 °C overnight.

The occluded organic was removed by heating the solid progressively from room temperature up to 580 °C and then maintaining this temperature for 6 h while changing the gas flow (100 cm<sup>3</sup>/min) from dry N<sub>2</sub> to air.

**Acknowledgment.** Financial support by the Spanish Ministry of Science and Technology (Grant MAT2003-01226) is gratefully acknowledged. P.A. and B.F. thank the Spanish Ministry of Science and Technology for a postgraduate research scholarship.

### References and Notes

- (1) Corma, A.; García, H. *Catal. Today* **1997**, *38*, 257.
- (2) Corma, A. *Chem. Rev.* **1995**, *95*, 559.
- (3) Corma, A.; García, H. *Chem. Rev.* **2002**, *102*, 3837.
- (4) Wittmann, A.; Nowotny, H.; Munster, N. *Monatsh. Chem.* **1959**, *90*, 7.
- (5) Bittner, H.; Hauser, E. *Monatsh. Chem.* **1970**, *101*, 1471.
- (6) Lerot, L.; Poncelet, G.; Fripiat, J. J. *Mater. Res. Bull.* **1974**, *9*, 979.
- (7) Poncelet, G.; Dubru, M. L.; Jacobs, P. A. *ACS Symp. Ser.* **1977**, *40*, 606.
- (8) Hauser, E.; Hoch, M. J. R. *J. Magn. Reson.* (1969–1992) **1973**, *10*, 211.
- (9) Blasco, T.; Corma, A.; Diaz-Cabanas, M. J.; Rey, F.; Vidal-Moya, J. A.; Zicovich-Wilson, C. M. *J. Phys. Chem. B* **2002**, *106*, 2634.
- (10) Corma, C. A.; Rey, G. F.; Navarro, V. M. T.; Valencia, V. S. (Consejo Superior De Investigaciones Científicas, Spain; Universidad Politécnica De Valencia). Synthesis of ITQ-17 in the Absence of Fluoride Ions. PCT Int. Appl. WO, 2003.
- (11) Corma, A.; Rey, F.; Valencia, S.; Jorda, J. L.; Rius, J. *Nature Mater.* **2003**, *2*, 493.
- (12) Plevet, J.; Gentz, T. M.; Laine, A.; Li, H.; Young, V. G.; Yaghi, O. M.; O'Keeffe, M. J. *Am. Chem. Soc.* **2001**, *123*, 12706.
- (13) Sastre, G.; Vidal-Moya, J. A.; Blasco, T.; Rius, J.; Jorda, J. L.; Navarro, M. T.; Rey, F.; Corma, A. *Angew. Chem., Int. Ed.* **2002**, *41*, 4722.
- (14) Scaiano, J. C.; García, H. *Acc. Chem. Res.* **1999**, *32*, 783.
- (15) García, H.; Roth, H. D. *Chem. Rev.* **2002**, *102*, 3947.
- (16) Hashimoto, S. J. *Photochem. Photobiol., C* **2003**, *4*, 19.
- (17) Anpo, M.; Yamashita, H. Photochemistry of Surface Species Anchored on Solid Surfaces. In *Surface Photochemistry*; Anpo, M., Ed.; John Wiley and Sons: Chichester, U.K., 1996; p 117.
- (18) Hays, G. R.; Van Erp, W. A.; Alma, N. C. M.; Couperus, P. A.; Huis, R.; Wilson, A. E. *Zeolites* **1984**, *4*, 377.
- (19) Cruz, J. M.; Corma, A.; Fornes, V. *Appl. Catal.* **1989**, *50*, 287.
- (20) Liu, S. B.; Wu, J. F.; Ma, L. J.; Tsai, T. C.; Wang, I. J. *Catal.* **1991**, *132*, 432.
- (21) Hong, Y.; Fripiat, J. J. *Microporous Mater.* **1995**, *4*, 323.
- (22) Campbell, S. M.; Bibby, D. M.; Coddington, J. M.; Howe, R. F.; Meinhold, R. H. *J. Catal.* **1996**, *161*, 338.
- (23) Deng, F.; Yue, Y.; Ye, C. *J. Phys. Chem. B* **1998**, *102*, 5252.
- (24) Corma, A.; Diaz-Cabanas, M. J.; García, H.; Palomares, E. *Chem. Commun.* **2001**, 2148.
- (25) Kelly, G.; Willsher, C. J.; Wilkinson, F.; Netto-Ferreira, J. C.; Olea, A.; Weir, D.; Johnston, L. J.; Scaiano, J. C. *Can. J. Chem.* **1990**, *68*, 812.
- (26) Bohne, C.; Redmond, R. W.; Scaiano, J. C. Use of the Photophysical Techniques in the Study of Organized Assemblies. In *Photochemistry in Organized and Constrained Media*; Ramamurthy, V., Ed.; VCH: New York, 1991; Chapter 3.
- (27) Moissette, A.; Vezin, H.; Gener, I.; Bremard, C. *J. Phys. Chem. B* **2003**, *107*, 8935.
- (28) Moissette, A.; Marquis, S.; Gener, I.; Bremard, C. *Phys. Chem. Chem. Phys.* **2002**, *4*, 5690.
- (29) Moissette, A.; Vezin, H.; Gener, I.; Patarin, J.; Bremard, C. *Angew. Chem., Int. Ed.* **2002**, *41*, 1241.
- (30) O'Neill, M. A.; Cozens, F. L.; Schepp, N. P. *J. Phys. Chem. B* **2001**, *105*, 12746.
- (31) Wilkinson, F.; Kelly, G. Diffuse Reflectance Flash Photolysis. In *Handbook of Organic Photochemistry*; Scaiano, J. C., Ed.; CRC Press: Boca Raton, FL, 1989; Vol. 1, p 293.